0022-3565/05/3141-431–436$20.00
THE JOURNAL OF PHARMACOLOGY AND EXPERIMENTAL THERAPEUTICS
Vol. 314, No. 1
85704/3038969
Printed in U.S.A.

JPET 314:431–436, 2005

Acute Inhibition of Cardiac Monoamine Oxidase A after Tobacco Smoke Inhalation: Validation Study of [^{11}C]Befloxatone in Rats Followed by a Positron Emission Tomography Application in Baboons

Héric Valette, Michel Bottlaender, Frédéric Dollé, Christine Coulon, Michèle Ottaviani, and André Syrota

Service Hospitalier Frédéric Joliot, Direction of Life Sciences, Department of Medical Research, French Atomic Agency, Orsay, France

Received March 3, 2005; accepted April 12, 2005

ABSTRACT

The in vivo characteristics of [^{11}C]befloxatone were assessed in myocardium of rats and monkeys. A complete multicompartmental model was developed to quantify monkey cardiac monoamine oxidase A (MAO-A) binding sites using positron emission tomography (PET) and was applied to assess the acute effects of inhalation of tobacco smoke. Unknown compounds contained in tobacco smoke inhibit brain MAO. In vitro, befloxatone inhibits selectively, competitively, and reversibly MAO-A in human tissues. [^{11}C]Befloxatone (1.85 MBq) was i.v. injected into rats. Animals were sacrificed, dissected, and samples were assessed for radioactivity. Another group of rats was pretreated with clorgyline (10 mg/kg i.v.). Monkeys were injected with [^{11}C]befloxatone (222–370 MBq), and the chest was imaged with PET for 2 h. Presaturation and displacement experiments were performed using unlabeled befloxatone. For quantification of myocardial binding sites (B_{max}), [^{11}C]befloxatone was first injected as a tracer dose (2.7–9.3 nmol) and 20 min later injected as a mixture of labeled and unlabeled befloxatone (labeled, 10.3–41.9 nmol; unlabeled, 407–765 nmol). In rodents, cardiac uptake was high (3.39 $\pm$ 0.5% injected dose/g tissue) and strongly inhibited (80%) by clorgyline. In monkeys, administration of unlabeled befloxatone displaced 85% of cardiac radioactivity. B_{max} was found to be 208 $\pm$ 13 pmol ml^{-1} tissue. Inhalation of tobacco smoke decreased B_{max}: 150 $\pm$ 6.2 pmol ml^{-1}, whereas nicotine did not. [^{11}C]Befloxatone allows a good visualization of the heart. Cardiac MAO-A B_{max} was quantified and a clear effect of acute inhalation of tobacco smoke was evidenced. Therefore, a single cigarette can interfere with the cardiac turnover of catecholamines.

MAO (monoamine: oxidoreductase deaminating EC 1.4.3.4) plays a key role in the metabolism of endogenous amines and xenobiotics. MAO has been subdivided into MAO-A and MAO-B subtypes according to substrate specificity (MAO-A: 5-hydroxytryptamine, norepinephrine, epinephrine, and serotonin; and MAO-B: phenylethylamine and benzylamine). MAO inhibitors are widely used for treatment of depression and tobacco addiction or tobacco weaning (Robinson 2002; Villegier et al., 2003). Therefore, in vivo study of MAO using PET has mainly focused on neuropsychiatric disorders or tobacco addiction. Smoking is a major public health problem. Although several pharmacological properties of nicotine are known, tobacco smoke contains about 4000 chemical compounds with unknown properties. Smokers have reduced levels of brain monoamine oxidase (Fowler et al., 1996a,b). Little in vivo data are available about myocardial MAO. In the heart, MAO-A is abundant (Saura et al., 1992). Active reuptake (uptake-1) metabolism of norepinephrine by MAO and by catechol-*O*-methyltransferase are the major ways for ending the action of the neurotransmitters (Eisenhofer et al., 2004).

In vivo MAO studies with PET involve the use of an inhibitor of the enzymes. The prototype inhibitors ("suicide inactivators", which engender covalent bonds with the active site of the enzyme and induce irreversible inhibition) used in PET studies are [^{11}C]deprenyl and [^{11}C]clorgyline (Fowler et al., 1996a,b), which inhibit MAO-B and MAO-A, respectively. They have been successfully used in humans with PET to demonstrate the inhibition of brain MAO-A and MAO-B in smokers. But these two inhibitors are known to exhibit a strong deuterium effect; therefore, their synthesis needs to have the deuterated precursors (Fowler et al., 1995).

Article, publication date, and citation information can be found at http://jpet.aspetjournals.org.
doi:10.1124/jpet.105.085704.

ABBREVIATIONS: MAO, monoamine oxidase; PET, positron emission tomography; i.d., injected dose; ANOVA, analysis of variance.

Among the second generation of reversible, highly selective MAO-A inhibitors, befloxatone inhibited competitively MAO-A in several human and rodent tissues with K_i values ranging from 1.9 to 3.6 nM (Curet et al., 1996). Its corresponding values for MAO-B were 270 to 900 nM (Curet et al., 1996). The ^{11}C-radiolabeled befloxatone (Dollé et al., 2003a,b) has been developed to study brain MAO-A and was fully characterized in baboons (Bottlaender et al., 2003). In whole-body scans, we have observed that both the human and baboon hearts were clearly seen (unpublished data). Therefore, pharmacological characterization of befloxatone cardiac uptake was performed in rats and in baboons. A compartmental model was applied to PET data to determine the left ventricular density of binding sites and to assess their acute changes induced by inhalation of tobacco smoke. As a consequence of a partial inhibition of cardiac MAO-A activity, the clearance of catecholamine could be reduced, altering the sympathetic tone and potentially contributing to some deleterious effects of smoking. Therefore, the PET study of MAO in the heart seems clinically relevant.

Materials and Methods

Radiosynthesis of [^{11}C]Befloxatone

Befloxatone [(5*R*)-5-(methoxymethyl)-3-[4-[(3*R*)-4,4,4-trifluoro-3-hydroxybutoxy] phenyl]-2-oxazolidinone] was labeled with ^{11}C from the ring-opened precursor (*R*)-1-methoxy-3-[[4-[(3*R*)-4,4,4-trifluoro-3-hydroxybutoxy]-phenyl]amino]-2-propanol using no-carrier-added [^{11}C]phosgene (Dollé et al., 2003a,b). Typically, starting from a 44.4 GBq cyclotron-produced [^{11}C]CH_4 batch, 5.55 to 11.10 GBq of [^{11}C]befloxatone with a radiochemical and chemical purity of more than 99% were routinely obtained within 20 min of radiosynthesis (including high-pressure liquid chromatography purification) with specific radioactivities of 18.5 to 74.0 GBq/μmol.

Animal Studies

Procedures used in rats and monkeys were in accordance with the recommendations of the European Economic Community (86/609/CEE) and the French National Committee (decret 87/848) for the care and use of laboratory animals.

Biodistribution in Rodents

Male Sprague-Dawley rats (average weight 200 g) were injected in a tail vein with 1.85 MBq of [^{11}C]befloxatone. Animals (n = 5 at each time point) were sacrificed 5, 10, and 30 min later and dissected, and the samples (blood, plasma, heart, liver, kidneys, lungs, and gastrocnemius) were weighed and assessed for radioactivity (gamma counter, model 5000; Amersham Biosciences Inc., Piscataway, NJ). Another group of animals (n = 5 at each time point) was pretreated with clorgyline (10 mg/kg i.v.) 1 h before the injection of [^{11}C]befloxatone and sacrificed 10 or 30 min later. Samples were processed as described above. All results are expressed as the percentage of injected dose per gram of wet tissue (% i.d./g tissue).

PET Characterization of [^{11}C]Befloxatone in Monkeys

PET studies of the thoracic distribution of [^{11}C]befloxatone were carried out in adult male *Papio anubis* baboons (mean weight 10 kg). The rest period between two PET scans was 2 weeks. Two hours before the PET acquisition, the animals received ketamine (10 mg/kg i.m.). After being intubated, animals were artificially ventilated and maintained anesthetized with 66% N_2O/1% isoflurane (ventilator OAV 7710; Ohmeda PPD, Liberty Corner, NJ). One catheter was placed in the femoral artery and another one in a sural vein. Animals were positioned in an Exact HR+ scanner (CTI PET Systems, Knoxville, TN), which is also suitable for cardiac imaging of small animals. This scanner allows simultaneous acquisition of 31 slices (3.37 mm apart) with an intrinsic spatial resolution of about 6 mm. Reconstructed images had a resolution of 8.5 mm. Transmission scans were acquired for 15 min using three retractable Germanium-68 rod sources and used for subsequent attenuation correction.

Baboons (n = 3) were injected i.v. with 222 to 370 MBq (12–18 nmol) of [^{11}C]befloxatone and imaged for 60 to 120 min according to the experimental protocol. During PET acquisition, arterial blood samples were withdrawn from a femoral artery at designated times. One PET experiment was performed to examine whether the [^{11}C]befloxatone myocardial uptake could be displaced by injecting, 60 min after the radiotracer, unlabeled befloxatone (0.4 mg/kg i.v; as a 1-min bolus). The PET imaging was continued for 60 min. A presaturation experiment was also performed using a dose of 0.4 mg/kg unlabeled befloxatone.

PET Data Processing

Myocardial time activity curves were measured from a left ventricular region of interest automatically drawn with an isocontour plotting routine. The 70% isocontour included both the interventricular septum and the left ventricular free wall. [^{11}C]Befloxatone tissue concentrations (Bq ml^{-1}) were obtained after correction for attenuation and for ^{11}C decay and expressed as picomoles per milliliter using the value of the specific radioactivity measured at the beginning of the PET experiment.

PET Studies for the Ligand-Binding Site Model

The multi-injection approach (see *The Ligand-Binding Site Model* section below) consists in performing several injections of labeled and/or unlabeled ligand. In this study, six PET experiments were performed on three baboons (Table 1). The total duration of the experiments was 80 min. The experimental protocol included two injections (slow bolus over 1 min): 1) a tracer (2.7–9.3 nmol; Table 1) injection of [^{11}C]befloxatone with a high specific radioactivity at the beginning of the experiment (time t_0 = 0), and 2) a coinjection of [^{11}C]befloxatone (10.3–41.9 nmol) and a large amount (407–765 nmol) of unlabeled befloxatone, 20 min after the beginning of the experiment. This protocol enabled the estimation of all model parameters (including the binding site concentration and the vascular fraction) by fitting the PET experimental curves through a minimization of the usual weighted least-square cost function.

Input Function

The identification of model parameters required the knowledge of the plasma unchanged radioligand concentration, which was used as the input function in the subsequent modeling. During the PET acquisition, arterial blood samples (0.5 ml) were withdrawn at designated times. Blood and plasma radioactivities were measured in a gamma counter, and the time-activity curves were corrected for ^{11}C decay from the time of the first injection. Blood samples (1 ml) for metabolite determination were collected at 10, 15, and 20 min after each injection of the tracer, immediately centrifuged to obtain cell free plasma, and processed as described previously (Bottlaender et al., 2003). Plasma concentration of unchanged radioligand was ex-

TABLE 1
Protocol parameters corresponding to the six control experiments

	Exp 1	Exp 2	Exp 3	Exp 4	Exp 5	Exp 6
First injection						
t_0 (min)						
Nanomoles labeled	4.70	9.35	3.80	2.89	2.71	7.76
Second injection						
t_{20} (min)						
Nanomoles labeled	21.60	41.96	16.4	13.27	10.30	29.74
Nanomoles unlabeled	630	630	629	407	430	765

pressed as picomoles per milliliter after division by the specific radioactivity measured at the beginning of the PET experiment.

Pharmacological Interventions

Inhalation of Tobacco Smoke. The PET experimental protocol (four experiments on two baboons) also included two injections of [^{11}C]befloxatone. Since a partial inhibition of MAO-A binding sites was expected after inhalation of tobacco smoke, the dose of unlabeled befloxatone was reduced to 449 to 505 nmol (Table 2). The "smoking" procedure was performed 10 to 15 min before the first injection of [^{11}C]befloxatone. For inhalation of tobacco smoke, a cigarette, containing 0.8 mg of nicotine, was connected to a syringe that was inserted into the inspiratory circuit, the expiratory circuit being opened to avoid the recirculation of smoke (Valette et al., 2003). Through the syringe, the baboon received three puffs (15 ml each) per minute for a total duration of 5 min. The puffs were mixed to the tidal volume (mean value = 120 ml) during inspiration. The ratio of inspiration/expiration duration was set and maintained at one-third during all the experiments.

Pretreatment with Intravenous Nicotine. The PET experimental protocol was the same as for control experiments (Table 3). Nicotine (0.6 mg i.v. as a 5-min bolus) was injected 10 to 15 min before the first injection of [^{11}C]befloxatone.

The Ligand-Binding Site Model

The compartmental model used in this study is based on the nonequilibrium nonlinear model (Delforge et al., 1989, 1993). It includes three compartments (and an eventual fourth compartment for nonspecific binding) and seven parameters (Fig. 1).

The flux of nonmetabolized free ligand from the plasma compartment to the free ligand compartment is given by $k_1\ C_a^*(t)$ (as picomoles per minute per milliliter of tissue), where $C_a^*(t)$ is the plasma concentration of nonmetabolized [^{11}C]befloxatone.

The quantity of free labeled ligand present in 1 ml of the tissue volume delineated by the PET region of interest is denoted by $M_f^*(t)$. However, because of the obvious heterogeneity of the tissue, this concentration can be heterogeneous in the region of interest. For example, the local concentration of the free ligand in the vicinity of the binding sites (which is the concentration to take into account in the ligand-receptor interactions) may be different from $M_f^*(t)$ (which, by definition, represents the mean concentration in the unit of volume measured by PET). To take into account this heterogeneity, the concept of the reaction volume (V_R, unit: milliliters per milliliter of tissue) was introduced previously (Delforge et al., 1996). The value of

TABLE 2
Protocol parameters corresponding to the four experiments after inhalation of tobacco smoke

	Exp 1	Exp 2	Exp 3	Exp 4
First injection				
t_0 (min)				
Nanomoles labeled	6.9	3.3	3.3	5.2
Second injection				
t_{20} (min)				
Nanomoles labeled	30.6	12.3	12	18.9
Nanomoles unlabeled	449	499	505	491

TABLE 3
Protocol parameters corresponding to the two experiments after injection of nicotine

	Exp 1	Exp 2
First injection		
t_0 (min)		
Nanomoles labeled	6.2	3.2
Second injection		
t_{20} (min)		
Nanomoles labeled	27	14
Nanomoles unlabeled	545	584

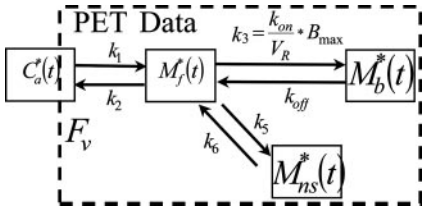

Fig. 1. Description of the compartmental model. $k_1 C_a^*(t)$ is the flux of nonmetabolized free ligand from the plasma compartment to the free ligand compartment. $M_f^*(t)$ is the concentration (present in 1 ml) of the free ligand in the region of interest. $M_b^*(t)$ is the bound ligand. $M_{ns}^*(t)$ is the nonspecifically bound ligand. k_1, k_2, k_3, k_{off}, k_5, and k_6 are the transfer constants.

V_R is such that $M^*(t)/V_R$ is equal to the local free ligand concentration in the vicinity of the binding sites. The free ligand can bind directly to a specific binding site (or to a nonspecific site) or escape back to the blood with a rate constant k_2.

The specific binding is a saturable reaction that depends on a bimolecular association rate constant, k_{on}; the free ligand concentration in the vicinity of the receptor sites, $M_f^*(t)/V_R$; and the quantity of binding sites (B_{max}) in 1 ml of tissue. This last quantity is equal to B_{max} which is the binding site concentration since the stoichiometry is 1 mol of inhibitor (befloxatone) per mole of enzyme (Ramsay and Hunter, 2002). The rate constant for the dissociation of the specifically bound ligand is denoted by k_{off}. The in vivo equilibrium dissociation rate constant is denoted by $k_d V_R$, where k_d is the ratio k_{off}/k_{on}.

The multi-injection protocol included injections of radioligand with addition of a large amount of unlabeled ligand. B_{max}, k_1, k_2, k_{on}/V_R, and k_{off} (and in the event k_5, and k_6 for the nonspecifically bound ligand) are the model parameters to be identified. Units are given in Table 4. The two parameters k_{on} and V_R cannot be estimated separately because they always occur together in model equations. In PET studies, the experimental data (denoted by $M_T^*(t_i)$ acquired between two time points (denoted by t_{i-1} and t_i) are given by the following integral relationship:

$$M_T^*(t_i) = \frac{1}{t_i - t_{i-1}} \int_{t_{t-1}}^{t_i} (M_f^*(t) + M_b^*(t) + F_V C_B^*(t)) dt$$

where $C_B^*(t)$ is the whole-blood time-concentration curve, and F_V represents the vascular volume that is the fraction of blood present in the tissue volume. In this study, F_V was fitted since it represented a large percentage of the myocardial tissue.

The model parameters are identified through a minimization of the usual weighted least-square cost function, and the estimation of the standard errors relies on a sensitivity analysis and on the covariance matrix (Delforge et al., 1989). Comparisons between model structures are based on the use of the Akaike information criterion (Akaike, 1974) and of the F-test (Akaike, 1974; Landaw and Di Stefano, 1984).

Statistical Analysis

Results are expressed as means ± S.D. Comparison of model parameters after pharmacological interventions was performed using ANOVA. A probability level of $p < 0.05$ was considered statistically significant.

Results

In rats, myocardial radioactivity slightly increased from 15 to 30 min with an uptake of 3.39 ± 0.5 and 3.8 ± 0.02% i.d./g tissue, respectively. Pretreatment with clorgyline reduced myocardial radioactivity by 85% at both 15 and 30 min postinjection.

In baboons, myocardial radioactivity plateaued at 5 min (Fig. 2). The uptake was high: 6% i.d./100 ml tissue at 20 min

postinjection. Clearance from the lung was rapid (Fig. 2); therefore, the ratio of heart to lung was 3.5 at 60 min. Injection of unlabeled befloxatone (0.4 mg/kg as a 1-min bolus at $t = 60$ min) displaced 80% of myocardial radioactivity in 1 h (Fig. 2). After injection of [^{11}C]befloxatone, radioactivity in the liver increased progressively, peaking at 50 to 60 min (9% i.d./100 ml tissue). Pretreatment with a large amount of unlabeled befloxatone (0.4 mg/kg) showed a large proportion of displaceable binding in the liver (65%; Fig. 3). The washout was slow, however; therefore, calculation of the percentage of nonspecific binding was not possible because of the short half-life of ^{11}C ($t_{1/2}$ of 20.4 min).

Results of high-pressure liquid chromatography showed that, 20 min after injection of a tracer dose of befloxatone, unchanged [^{11}C]befloxatone represented 96 ± 6% of plasma radioactivity. On the contrary, 20 min after a coinjection of labeled and unlabeled befloxatone, unchanged [^{11}C]befloxatone represented 80 ± 11 and 65 ± 11% of plasma radioactivity, at 40 min postinjection (Fig. 4).

Parameter Identification in Control Experiments. Fitting the complete mathematical model to experimental data provided values for kinetic rate constants and binding site density. The numerical values are shown in Table 4. The quality of the fits was satisfactory in all experiments as can be seen in Fig. 5. The relative standard errors were small for the parameters excepted for k_{on}/V_R and k_{off} (Table 4). Average binding site density was 208 ± 13 pmol ml^{-1} tissue. Introduction into the model of a compartment with nonspecifically bound ligand did not improve the quality of the fits (data not shown). Myocardial time-activity curves for free and bound ligand were calculated for the six experiments by using the parameter values shown in Table 4. Figure 6 shows the quality of the fit and the result of simulation obtained with the parameters estimated from experiment 2.

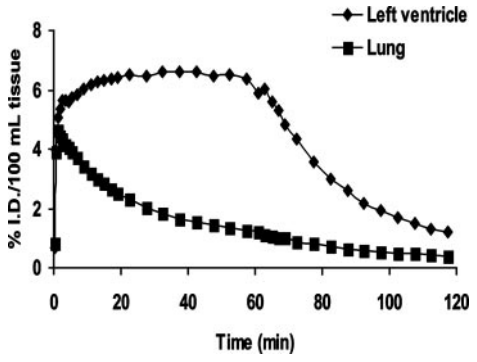

Fig. 2. Left ventricular and lung time activity curves in a baboon. Unlabeled befloxatone (0.4 mg/kg) was i.v. injected at 60 min. At least 80% of myocardial radioactivity is displaced by unlabeled ligand.

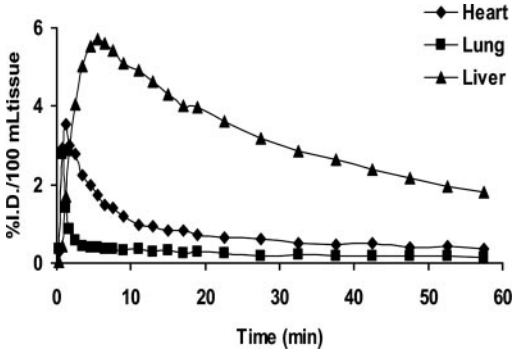

Fig. 3. Pretreatment with unlabeled befloxatone (0.4 mg/kg). The myocardial time-activity curve shows a steep washout reaching a low level in 20 min, indicating a low percentage of nonspecific binding.

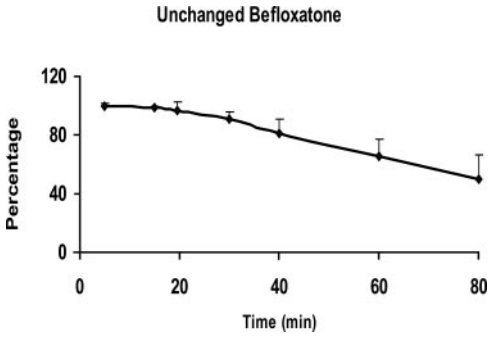

Fig. 4. Unchanged befloxatone in plasma. After a tracer injection of [^{11}C]befloxatone, the metabolism is negligible (time 0–20 min). After a coinjection (at 20 min) of a mixture of [^{11}C]befloxatone and several 100 nmol of unlabeled befloxatone, metabolism of befloxatone is rapid.

Parameter Identification after Pharmacological Interventions. After inhalation of tobacco smoke, a significant (ANOVA, $p = 0.03$) decrease in density in binding sites was observed in all animals. Average binding site density was 150 ± 6.2 pmol ml^{-1} tissue (Table 5). No change in left ventricular blood flow (estimated by k_1) was observed (control value: 0.5 ± 0.15 min^{-1}, inhalation of tobacco smoke 0.5 ± 0.11 min^{-1}, ANOVA, $p = 0.1$). Estimates of association ($k_{on}V_R$) and dissociation (k_{off}) constants were slightly increased (ANOVA, $p = 0.3$) and slightly decreased (ANOVA, $p = 0.2$), respectively, after inhalation of tobacco smoke (Tables 2 and 4). Their ratio (k_d/V_R) was slightly decreased (ANOVA, $p = 0.4$).

Nicotine injection did not affect the density of binding sites (ANOVA, $p = 0.5$; Table 6). Left ventricular blood flow (estimated by k_1), k_{on}/V_R and k_{off} were slightly increased (ANOVA, $p > 0.1$ for all three parameters; control values in Table 4).

Discussion

Although the cardiac uptake-one carrier is considered as the main way of ending the pharmacological effects of catecholamines, enzymatic degradation by MAO-A and -B plays a crucial role in the regulation of tissue levels of serotonin, norepinephrine, epinephrine, and dopamine. At the cardiovascular level, the functions of MAOs were clearly evidenced in MAO-A/B-deficient mice (Holschneider et al., 2002a,b). In these animals, both heart rate dynamics and baroreceptor responses were strongly altered. Smoking exposes the brain and the peripheral organs to unidentified substances that inhibit both MAOs (Fowler et al., 1996a,b, 2003a,b). The reduced clearance of catecholamine in peripheral organs, such as the liver and the gastrointestinal tract, could alter the sympathetic tone and potentially contribute to some deleterious effects of smoking. Therefore, the PET study of MAO in the heart seems clinically relevant.

[^{11}C]Befloxatone, a selective, reversible MAO-A ligand was first developed to study with PET the cerebral monoamine oxidase (Dollé et al., 2003b). On the whole-body images performed in humans and baboons, the heart was clearly visualized in spite of the short time frame (1 min)

TABLE 4
Model parameters identified from experimental data obtained (protocol described in Table 1)

	Exp 1	Exp 2	Exp 3	Exp 4	Exp 5	Exp 6	Mean ± S.D.
B_{max} (pmol ml^{-1})	199	202	191	224	214	222	208 ± 13.3
k_1 (min^{-1})	0.75	0.60	0.43	0.47	0.43	0.34	0.50 ± 0.15
k_2 (min^{-1})	0.91	0.92	1.08	1.19	1.43	0.82	0.99 ± 0.34
k_{on}/V_R (ml pmol^{-1} min^{-1})	0.022	0.037	0.046	0.033	0.036	0.033	0.034 ± 0.01
k_{off} (min^{-1})	0.049	0.068	0.10	0.10	0.054	0.047	0.069 ± 0.02
F_V (ml)	0.23	0.21	0.28	0.46	0.32	0.39	0.31 ± 0.1
$k_d V_R$ (nM/ml)	2.23	1.84	2.17	3.03	1.5	1.44	2.03 ± 0.59

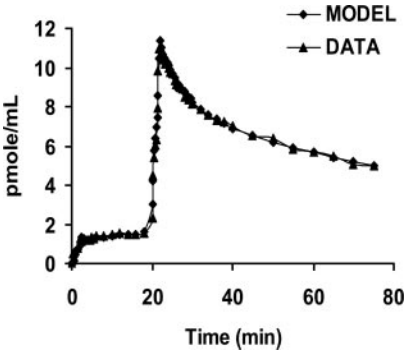

Fig. 5. Left ventricular time activity curve and fit of the PET data using the compartmental model. The experimental protocol is described in Table 1 (experiment 2).

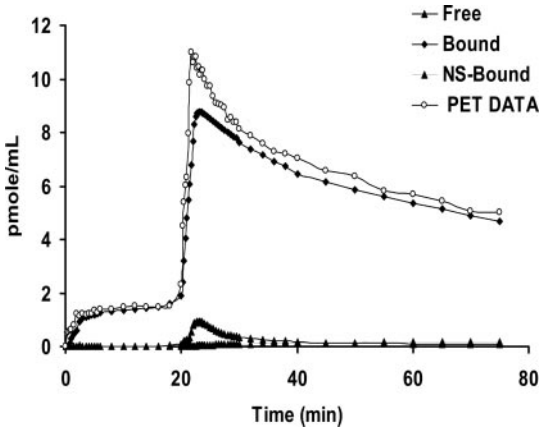

Fig. 6. Simulation of free, bound, nonspecifically bound ligand, and experimental PET data (experiment 2). The presence of nonspecifically bound ligand is transient (from 20 to 30 min) after the coinjection of [^{11}C]befloxatone and several 100 nmol of unlabeled befloxatone.

of the images (unpublished data). Therefore, the present preliminary study was undertaken in rats to validate the use of [^{11}C]befloxatone for the visualization of cardiac MAO-A. In rat heart, MAO-A is abundant and the enzymatic activity is 2-fold higher than that of lungs (Saura et al., 1992). [^{11}C]Befloxatone left ventricular uptake was 4 times higher than lung uptake, suggesting the ability of befloxatone to visualize the myocardium. Presaturation studies with clorgyline demonstrated the specificity of the befloxatone binding to the cardiac tissue. As a further step, myocardial binding of befloxatone was studied in monkeys. Plasma clearance of the radiotracer was rapid. Metabolism of befloxatone, at a tracer dose, was slow (Bottlaender et al., 2003). In contrast, after the injection of 100 nmol of befloxatone, the metabolism of the tracer was far from negligible. Myocardial kinetics of befloxatone was rapid. Presaturation and displacement experiments demonstrated the specificity and the reversibility of the cardiac binding of befloxatone. The high-contrast heart/lung, 50-min postinjection makes befloxatone an excellent ligand for the visualization of cardiac MAO-A. The multi-injection protocol allowed the estimation of all parameters of the model, although standard errors of the estimates were rather large for two parameters: k_{on}/V_R and k_{off}.

In the present study, the B_{max} of cardiac MAO-A was reduced after inhalation of smoke of a single cigarette, whereas injection of nicotine had no significant effect. Both MAO-A and MAO-B are reduced in animals exposed to tobacco smoke (Yu and Boulton, 1987; Carr and Basham, 1991). In humans, reduced MAO-A and MAO-B activities were observed in heavy smokers (Berlin et al., 1995). Using PET, low brain MAO-A and low MAO-B in peripheral organs have been described previously (Fowler et al., 2003a,b). The same PET group has demonstrated that smoking a single cigarette (in humans) or nicotine alone (in baboons) did not change brain MAO-B activity (Fowler et al., 1998, 1999). Moreover, in chronic smokers, there was no change in myocardial MAO-A activity using [^{11}C]clorgyline (Fowler et al., 2004b). These discrepant results could be explained by several factors. The affinity of clorgyline for MAO-A is much less than that of befloxatone (Curet et al., 1996; Mukherjee and Yang, 1999). Clorgyline and befloxatone behave differently in vivo. In humans, [^{11}C]clorgyline has a higher binding to lung compared with heart (ratio close to 1; Fowler et al., 2004a), whereas the opposite is observed for befloxatone (ratio close to 4; unpublished data). Binding to the human heart is 0.015% i.d./ml tissue for befloxatone (unpublished data), whereas for clorgyline binding is 0.006% i.d./ml tissue (Fowler et al., 2004a). MAO-A activity (Fowler et al., 2004a) is estimated by λk_3 (with $\lambda = k_1/k_2$) for clorgyline, whereas we have developed a complete compartmental model that allows estimation of all parameters.

Activation of receptors in the brain and in peripheral tissues by nicotine results in the release of catecholamines (Benowitz, 1988). Both inhalation of tobacco smoke or infused nicotine increase heart rate and blood pressure. These cardiovascular effects are due to activation of nicotinic acetylcholine receptors located on postganglionic sympathetic nerve endings or on the adrenal medulla. This activation induces a release of epinephrine (and norepinephrine). Nicotine contained in tobacco smoke induced enhanced sympathetic tone, and other substances contained in tobacco smoke reduced cardiac MAO-A activity. Both factors may contribute to some deleterious effects of smoking. This is consistent with the observation of reduced catecholamine metabolites in smokers (Berlin et al., 1995).

TABLE 5
Model parameters identified from experimental data after inhalation of tobacco smoke (protocol described in Table 2)

	Exp 1	Exp 2	Exp 3	Exp 4	Mean ± S.D.
B_{max} (pmol ml^{-1})	146	139	153	151	150 ± 6.2
k_1 (min^{-1})	0.66	0.56	0.41	0.43	0.5 ± 0.11
k_2 (min^{-1})	1.92	0.53	1.34	0.56	1.08 ± 0.67
k_{on}/V_R (ml pmol^{-1} min^{-1})	0.036	0.056	0.077	0.05	0.055 ± 0.017
k_{off} (min^{-1})	0.036	0.04	0.038	0.036	0.025 ± 0.009
F_V (ml)	0.38	0.4	0.3	0.35	0.34 ± 0.04
k_dV_R (nM/ml)	1.2	1.5	2.1	1.55	1.59 ± 0.37

TABLE 6
Model parameters identified from experimental data after injection of nicotine (protocol described in Table 3)

	Exp 1	Exp 2	Mean ± S.D.
B_{max} (pmol ml^{-1})	225	213	219 ± 8.48
k_1 (min^{-1})	0.62	0.71	0.66 ± 0.06
k_2 (min^{-1})	0.95	0.4	0.67 ± 0.39
k_{on}/V_R (ml pmol^{-1} min^{-1})	0.04	0.065	0.05 ± 0.017
k_{off} (min^{-1})	0.13	0.066	0.098 ± 0.04
F_V (ml)	0.34	0.26	0.3 ± 0.05
k_dV_R (nM/ml)	3.25	1.01	2.13 ± 1.58

Conclusions

The use of [^{11}C]befloxatone, a selective, reversible MAO-A inhibitor, was validated in rats and monkeys for the visualization of the cardiac MAO-A. A protocol for the quantification of the density of myocardial MAO-A binding sites was developed in monkeys using PET, injections of [^{11}C]befloxatone, and unlabeled befloxatone and a multicompartmental analysis of the PET data. Inhalation of tobacco smoke (one single cigarette) acutely decreased the density of MAO-A binding sites, whereas nicotine alone did not. After tobacco smoke inhalation, acute changes in plasma epinephrine concentration (increased secretion by adrenal glands due to nicotine and reduced clearance due to cardiac MAO-A inhibition by unknown compounds contained in tobacco smoke) may have implications for both intravascular thrombosis (Badimon et al., 1999) and cardiac arrhythmias (Tisdale et al., 1995).

References

Akaike H (1974) A new look at the statistical model identification. *IEEE Trans Autom Contr* **19:**716–723.

Badimon L, Martinez-Gonzalez J, Royo T, Lassila R, and Badimon JJ (1999) A sudden increase in plasma epinephrine levels transiently enhances platelet deposition on severely damaged arterial wall–studies in a porcine model. *Thromb Haemost* **82:**1736–1742.

Benowitz NL (1988) Drug therapy. Pharmacologic aspects of cigarette smoking and nicotine addiction. *N Engl J Med* **319:**1318–1330.

Berlin I, Said S, Spreux-Varoquaux O, Olivares R, Launay JM, and Puech AJ (1995) Monoamine oxidase A and B activities in heavy smokers. *Biol Psychiatry* **38:**756–761.

Bottlaender M, Dolle F, Guenther I, Roumenov D, Fuseau C, Bramoulle Y, Curet O, Jegham J, Pinquier JL, George P, et al. (2003) Mapping the cerebral monoamine oxidase type A: positron emission tomography characterization of the reversible selective inhibitor [^{11}C]befloxatone. *J Pharmacol Exp Ther* **305:**467–473.

Carr LA and Basham JK (1991) Effects of tobacco smoke constituents on MPTP-induced toxicity and monoamine oxidase activity in the mouse brain. *Life Sci* **48:**1173–1177.

Curet O, Damoiseau G, Aubin N, Sontag N, Rovei V, and Jarreaux FX (1996) Befloxatone, a new reversible and selective monoamine oxidase-A inhibitor. Biochemical profile. *J Pharmacol Exp Ther* **277:**253–264.

Delforge J, Syrota A, and Bendriem B (1996) Concept of reaction volume in the in vivo ligand-receptor model. *J Nucl Med* **37:**118–125.

Delforge J, Syrota A, Bottlaender M, Varastet M, Loc'h C, Bendriem B, Crouzel C, Brouillet E, and Maziere M (1993) Modeling analysis of [^{11}C] flumazenil studied by PET: application to a critical study of the equilibrium approaches. *J Cereb Blood Flow Metab* **13:**454–468.

Delforge J, Syrota A, and Mazoyer BM (1989) Experimental design optimization: theory and application to estimation of receptor model parameters using dynamic positron emission tomography. *Phys Med Biol* **34:**419–435.

Dollé F, Bramoullé Y, Hinnen F, Demphel S, George P, and Bottlaender M (2003a) Efficient synthesis of [^{11}C]befloxatone, a selective radioligand for the in vivo imaging of MAO-A density using PET. *J Labelled Compd Radiopharm* **46:**783–792.

Dollé F, Valette H, Bramoulle Y, Guenther I, Fuseau C, Coulon C, Lartizien C, Jegham S, George P, Curet O, et al. (2003b) Synthesis and in vivo imaging properties of [^{11}C]befloxatone: a novel highly potent positron emission tomography ligand for mono-amine oxidase-A. *Bioorg Med Chem Lett* **13:**1771–1775.

Eisenhofer G, Kopin IJ, and Goldstein DS (2004) Catecholamine metabolism: a contemporary view with implications for physiology and medicine. *Pharmacol Rev* **56:**331–339.

Fowler JS, Logan J, Wang GJ, Franceschi D, Volkow ND, Telang F, Pappas N, Ferrieri R, Shea C, Garza V, et al. (2003a) Monoamine oxidase A imaging in peripheral organs in healthy human subjects. *Synapse* **49:**178–187.

Fowler JS, Logan J, Wang GJ, Volkow ND, Telang F, Ding YS, Shea C, Garza V, Xu Y, Li Z, et al. (2004a) Comparison of the binding of the irreversible monoamine oxidase tracers, [^{11}C]clorgyline and [^{11}C]deprenyl in brain and peripheral organs in humans. *Nucl Med Biol* **31:**313–319.

Fowler JS, Logan J, Wang GJ, Volkow ND, Telang F, Zhu W, Franceschi D, Pappas N, Ferrieri R, Shea C, et al. (2003b) Low monoamine oxidase B in peripheral organs in smokers. *Proc Natl Acad Sci USA* **100:**11600–11605.

Fowler JS, Volkow ND, Logan J, Pappas N, King P, MacGregor R, Shea C, Garza V, and Gatley SJ (1998) An acute dose of nicotine does not inhibit MAO B in baboon brain in vivo. *Life Sci* **63:**PL19–PL23.

Fowler JS, Volkow ND, Wang GJ, Pappas N, Logan J, MacGregor R, Alexoff D, Shea C, Schlyer D, Wolf AP, et al. (1996a) Inhibition of monoamine oxidase B in the brain of smokers. *Nature (Lond)* **379:**733–736.

Fowler JS, Volkow ND, Wang GJ, Pappas N, Logan J, Shea C, Alexoff D, MacGregor RR, Schlyer DJ, Zezulkova I, et al. (1996b) Brain monoamine oxidase A inhibition in cigarette smokers. *Proc Natl Acad Sci USA* **93:**14065–14069.

Fowler JS, Wang GJ, Logan J, Xie S, Volkow ND, MacGregor RR, Schlyer DJ, Pappas N, Alexoff DL, and Patlak C (1995) Selective reduction of radiotracer trapping by deuterium substitution: comparison of carbon-11-L-deprenyl and carbon-11-deprenyl-D2 for MAO B mapping. *J Nucl Med* **36:**1255–1262.

Fowler JS, Wang GJ, Telang F, Logan J, Shea C, Garza V, Xu Y, Ding YS, Alexoff D, Ferrieri RA, et al. (2004b) Comparison of MAO A in peripheral organs in nonsmokers and smokers (Abstract), in *Proceedings of the 51st Annual Meeting of the Society of Nuclear Medicine*; 2004 June 19–23; Philadelphia, PA. p 70.

Fowler JS, Wang GJ, Volkow ND, Franceschi D, Logan J, Pappas N, Shea C, MacGregor RR, and Garza V (1999) Smoking a single cigarette does not produce a measurable reduction in brain MAO B in non-smokers. *Nicotine Tob Res* **1:**325–329.

Holschneider DP, Scremin OU, Chialvo DR, Chen K, and Shih JC (2002a) Heart rate dynamics in monoamine oxidase-A- and -B-deficient mice. *Am J Physiol* **282:**H1751–H1759.

Holschneider DP, Scremin OU, Roos KP, Chialvo DR, Chen K, and Shih JC (2002b) Increased baroreceptor response in mice deficient in monoamine oxidase A and B. *Am J Physiol* **282:**H964–H972.

Landaw E and Di Stefano J (1984) Multiexponential, multicompartmental and non-compartmental modeling: data analysis and statistical considerations. *Am J Physiol* **246:**R665–R677.

Mukherjee J and Yang ZY (1999) Monoamine oxidase A inhibition by fluoxetine: an in vitro and in vivo study. *Synapse* **31:**285–289.

Ramsay RR and Hunter DJ (2002) Inhibitors alter the spectrum and redox properties of monoamine oxidase A. *Biochim Biophys Acta* **1601:**178–184.

Robinson DS (2002) Monoamine oxidase inhibitors: a new generation. *Psychopharmacol Bull* **36:**124–138.

Saura J, Kettler R, Da Prada M, and Richards JG (1992) Quantitative enzyme radioautography with 3H-Ro 411049 and 3H-Ro 196327 in vitro: localization and abundance of MAO-A and MAO-B in rat CNS, peripheral organs and human brain. *J Neurosci* **12:**1977–1999.

Tisdale JE, Patel RV, Webb CR, Borzak S, and Zarowitz BJ (1995) Proarrhythmic effects of intravenous vasopressors. *Ann Pharmacother* **29:**269–281.

Valette H, Bottlaender M, Dollé F, Coulon C, Ottaviani M, and Syrota A (2003) Long-lasting occupancy of central nicotinic acetylcholine receptors after smoking: a PET study in monkeys. *J Neurochem* **84:**105–111.

Villegier AS, Blanc G, Glowinski J, and Tassin JP (2003) Transient behavioral sensitization to nicotine becomes long-lasting with monoamine oxidases inhibitors. *Pharmacol Biochem Behav* **76:**267–274.

Yu PH and Boulton AA (1987) Irreversible inhibition of monoamine oxidase by some components of cigarette smoke. *Life Sci* **41:**675–682.

Address correspondence to: Dr. H. Valette, Service Hospitalier Frédéric Joliot, DSV/DRM-CEA, 4 Place du Général Leclerc, F-91406 Orsay, France. E-mail: valette@shfj.cea.fr